

# Orbital Acceleration Research Experiment: Calibration Measurements

Robert C. Blanchard\*

NASA Langley Research Center, Hampton, Virginia 23681-0001

John Y. Nicholson†

ViGYAN, Inc., Hampton, Virginia 23666-1325

and

James R. Ritter‡ and Kevin T. Larman§

Lockheed Engineering and Sciences Company, Inc., Hampton, Virginia 23666-1339

The Orbital Acceleration Research Experiment (OARE), which has flown on STS-40, STS-50, and STS-58, contains a three-axis accelerometer with a single, nonpendulous, electrostatically suspended proofmass, which can resolve accelerations to the  $10^{-9}$  g level. The experiment also contains a full calibration station to permit in situ bias and scale-factor calibration. This on-orbit calibration capability eliminates the large uncertainty of ground-based calibrations encountered with accelerometers flown in the past on the Orbiter, and thus provides absolute acceleration measurement accuracy heretofore unachievable. This is the first time accelerometer scale-factor measurements have been performed on orbit. A detailed analysis of the calibration process is given, along with results of the calibration factors from the on-orbit OARE flight measurements on STS-58. In addition, the analysis of OARE flight-maneuver data used to validate the scale-factor measurements in the sensor's most sensitive range are also presented. Estimates on calibration uncertainties are discussed. These uncertainty estimates provides bounds on the STS-58 absolute acceleration measurements for future applications.

## Nomenclature

$A$	= acceleration component
$\mathbf{A}$	= acceleration vector
$B$	= bias
$g$	= gravitational acceleration, 9.80665 m/s <sup>2</sup>
$ng$	= $10^{-9}$ g
$\mathbf{r}$	= distance vector
SF	= scale-factor ratio; see Eq. (1)
$X, Y, Z$	= sensor, body, or Orbiter axes
$\mu g$	= $10^{-6}$ g
$\omega$	= body-rate magnitude
$\boldsymbol{\omega}$	= body-rate vector
$\boldsymbol{\omega}_S$	= calibration table rotation rate vector
$\dot{\boldsymbol{\omega}}$	= angular acceleration vector

## Subscripts

aero	= aerodynamic components
b	= body axes
gg	= gravity-gradient components
O	= Orbiter reference axes
oop	= out-of-plane components
theor	= theoretical

## Introduction

THE Orbital Acceleration Research Experiment<sup>1</sup> (OARE) contains a triaxial accelerometer that uses a single free-floating (nonpendulous) electrostatically suspended cylindrical proofmass. The accelerometer sensor assembly is mounted to a microprocessor-

controlled, dual-gimbal platform in order to perform in-flight calibrations. Acceleration measurements are processed and stored in the OARE flight computer memory, and the unprocessed data are recorded simultaneously on the shuttle payload tape recorder. These tape-recorder data are telemetered periodically to ground stations during flight. The OARE is the third-generation Orbiter Experiment (OEX) Program accelerometer package. The OARE capabilities exceed both the Aerodynamic Coefficient Identification Package<sup>2</sup> (ACIP) and the High Resolution Accelerometer Package<sup>3</sup> (HiRAP) in sensitivity and performance.

The objective of OARE is to measure Orbiter aerodynamic performance on orbit, and thus it is purposely designed for low-frequency signals only. As the low-frequency acceleration environment of the Orbiter contains a variety of components, measurements or models of these components embedded in the acceleration measurements are required in order to extract the Orbiter aerodynamic acceleration signal. The models and measurements required to separate the components of low-frequency acceleration are discussed in Ref. 4.

There are several features that make the OARE desirable for making low-frequency acceleration measurements. One unique design feature of the OARE equipment is its ability to perform both bias and scale-factor calibrations on orbit. The OARE is the first accelerometer flight equipment to use in-flight scale-factor capabilities. Another experiment design feature is the OARE sensor, which is a nonpendulous accelerometer. Pendulous accelerometers, such as HiRAP, do not readily lend themselves to calibration on orbit, because they are highly temperature-sensitive in the  $10^{-6}$  g range. In the past, pendulous accelerometers have depended upon ground calibrations. Experience has shown ground calibration to be unreliable in predicting absolute bias on orbit.<sup>5</sup> Consequently, these accelerometers are unable to measure absolute acceleration signals with predictable accuracy. Therefore, OARE stands alone in its ability to establish precise absolute accelerations on orbit. Such measurements, in addition to extracting Orbiter rarefied-flow aerodynamic performance, are also crucial in characterizing the low-frequency environment for many experiments on the Orbiter, such as those involving electrophoresis, diffusion, and crystal growth.<sup>6</sup> These experiments are performed by a variety of national and international researchers.<sup>7-9</sup> The need to know the Orbiter vehicle microgravity environment is well documented in the literature.<sup>6,10</sup>

Received Aug. 2, 1994; revision received Nov. 21, 1994; accepted for publication Nov. 22, 1994. Copyright © 1994 by the American Institute of Aeronautics and Astronautics, Inc. No copyright is asserted in the United States under Title 17, U.S. Code. The U.S. Government has a royalty-free license to exercise all rights under the copyright claimed herein for Governmental purposes. All other rights are reserved by the copyright owner.

\*Senior Research Engineer, Mail Stop 408A. Associate Fellow AIAA.

†Senior Scientist.

‡Engineer.

§Senior Engineer. Member AIAA.

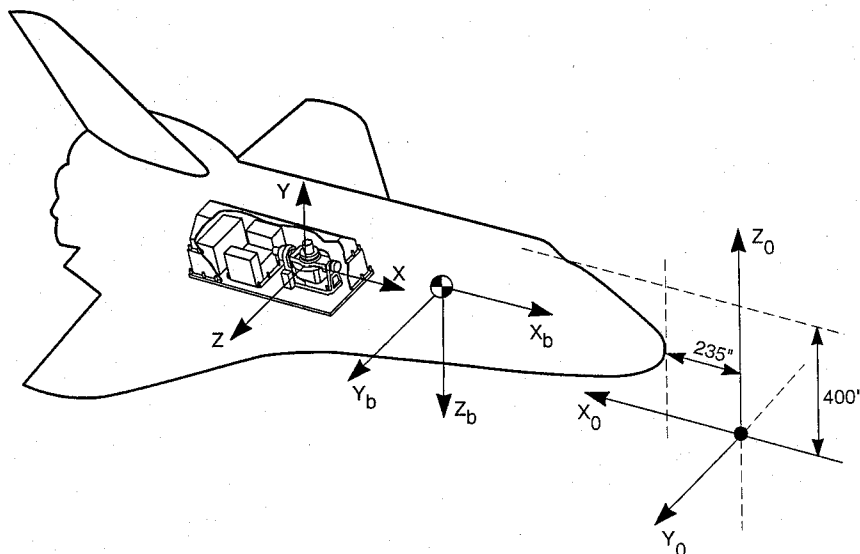


Fig. 1 Coordinate systems: OARE ( $X, Y, Z$ ), body axes ( $X_b, Y_b, Z_b$ ), and Orbiter reference ( $X_0, Y_0, Z_0$ ).

The initial development flight of the OARE equipment was on Shuttle mission STS-40.<sup>11</sup> This flight was followed by a second developmental flight, STS-50.<sup>12</sup> The OARE was flown a third time on Shuttle mission STS-58. This paper provides an in-depth discussion and analysis of the bias and scale-factor calibrations performed during the orbital portion of this flight. The article concentrates on biases and scale factors for only the most sensitive instrument range, since this is the applicable range while in orbit. In addition, this article provides the analysis of the three sets of flight maneuvers and the extraction of the scale factors for each axis from these maneuvers.

### Instrument Overview

Three coordinate systems are used in this article. Figure 1 shows schematically the three coordinate systems in relation to one another. The OARE coordinate system ( $X, Y, Z$ ) corresponds to the input axes of the OARE sensor in its reference position, and the origin is at the center of the proofmass. The standard aircraft body axis system ( $X_b, Y_b, Z_b$ ), whose origin is located at the Orbiter's center of gravity, and the Orbiter reference system<sup>13</sup> ( $X_0, Y_0, Z_0$ ) are also used. Units of inches are used in the Orbiter reference system in accordance with accepted Shuttle Project Office practices.

Figure 2 is a schematic of OARE, showing the various instrument components. The package is  $43.2 \times 33 \times 104.1$  cm ( $17 \times 13 \times 41$  in.) and is mounted on a keel bridge at bay 11 on the cargo-bay floor. The OARE sensor axes are coaligned with the Orbiter body axes as shown on Fig. 1. The instrument weighs 53.2 kg (117 lb) and requires 110 W of power. Three line replaceable units (LRUs) are mounted to a keel-bridge mounting plate. The three LRUs consist of the following: 1) the calibration table and sensor package, 2) the interface electronics, power system, and servo control modules, and 3) the 16-bit programmable microcomputer and memory. The accelerometer sensor is attached to a movable platform. The platform is rotated about two axes by two brushless dc torque motors.

Table 1 provides the sensor ranges, resolutions, and scale-factor calibration signals. There are three sensor ranges, A, B, and C, which correspond to acceleration scales for the X axis of  $\pm 10,000$ ,  $\pm 1000$ , and  $\pm 100 \mu g$ , respectively. The Y and Z axes are slightly different from X on account of the proofmass cylindrical design. The resolution in each axis and range is also given in Table 1. The best resolution of the sensor is  $3.05 \times 10^{-9} g$ , which is along the X axis. Table 1 also shows the scale-factor calibration signals, which range from 20 to 1392  $\mu g$  depending upon the table angular rate. There are two rates per range to check sensor linearity. In addition, the calibration platform moves in two angular directions, forward and reverse, for each axis of rotation in order to resolve platform motion characteristics.

Table 1 OARE sensor range, resolution, and scale-factor calibration signals

Range and resolution		
Range	Full scale, $10^{-6} g$	
	X axis	Y, Z axes
A	10000	25000
B	1000	1970
C	100	150
Range	Resolution, $10^{-9} g$	
	X axis	Y, Z axes
A	305.00	763.0
B	30.50	58.0
C	3.05	4.6
Scale-factor calibration		
Range	Cal. signals, $\mu g$	Data collection time, s
	X axis	
A	850.7	7.0
	425.3	11.0
B	850.7	6.7
	425.3	10.7
C	45.02	21.5
	20.01	32.2
Range	Y, Z axes	
A	1392.1	7.0
	695.9	11.0
B	1207.6	7.4
	530.6	12.6
C	67.2	22.5
	49.5	26.5

### In-Flight Calibration

#### Overview of the Calibration Station

OARE bias and scale-factor calibration data are acquired in flight using a computer-controlled, dual-gimbal rotary platform, referred to as the calibration station. The OARE calibration-table assembly is shown in Fig. 2 in front of the three electronic boxes. The inner gimbal motor moves the sensor package attached to the platform around the inner gimbal axis to stimulate the X-axis sensor or to orient the sensor input axis in a desired direction. This motion is accomplished using a 16-bit optical encoder to control the platform position. Known acceleration signals can be generated to determine scale factors simply by rotating the platform at a known constant rate. In addition, biases can be determined by orienting the

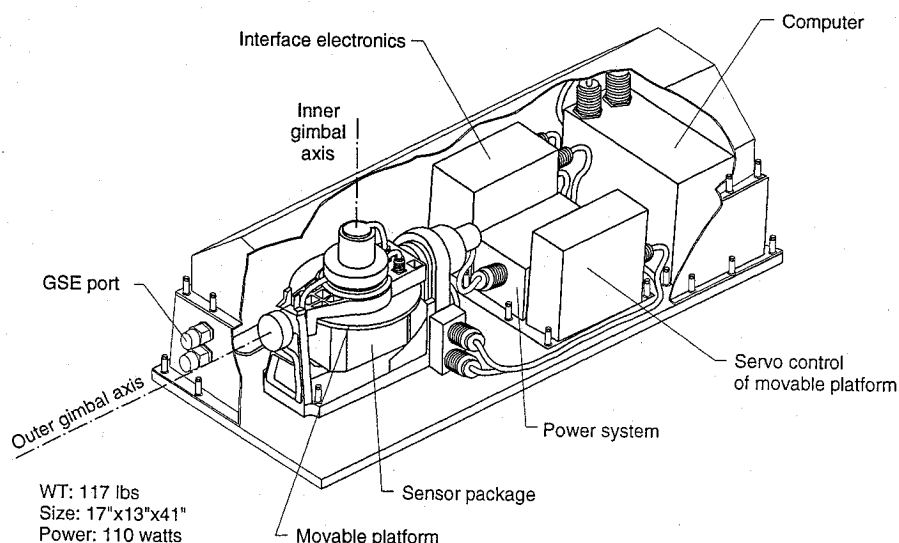


Fig. 2 Sketch of OARE packing layout.

input axes 180 deg apart, similar to a dividing head used in most accelerometer calibration laboratories. The outer gimbal motor provides a similar function for the  $Y$  and  $Z$  axes. Both of these input axes are simultaneously stimulated during rotation about the outer gimbal axis.

#### Calibration Process

The OARE sensor, like all accelerometers, is affected by manufacturing tolerances and variances in the physical environment including temperature and humidity, by its own inherent electronic drift, and by degradation of electronic components over time. These factors all impose a slowly changing acceleration signal. Because of this changing signal, periodic bias and scale-factor determinations are required to assure instrument accuracy.

Prior to flight, the bias and scale-factor measurements are scheduled at definite time intervals and programmed into the computer. Together, the biases and scale factors determined from the measurements are used to obtain an absolute reference for the measured signal. Bias determination is handled through scheduled reorientations of the sensor; scale-factor calibrations are handled through rate-controlled rotations. The bias measurement accounts for the instrument offset measured when no signal is present, and the scale factor provides a means to scale the output signal across the measurement range of the instrument. Since OARE has three measurement ranges, the biases and scale factors are determined for each of the ranges  $A$ ,  $B$ , and  $C$  for each of the three axes. The following two sections provide a general description of the bias and scale-factor calibration processes.

#### Bias Calibration

A bias measurement for the  $X$  axis is accomplished by taking a measurement at 0-deg inner-gimbal angle (the normal position), rotating the sensor 180 deg, and comparing the measurements made at 0 deg. The sum of these measurements yields twice the bias, while the difference is twice the input signal. Repeating this process for rotations around the outer-gimbal axis provides bias data for the  $Y$  and  $Z$  axes. In flight, the total bias calibration takes 8 to 10 min (three axes, three ranges) and is performed periodically throughout the mission. A set of 500 data points is collected in each position for each axis for each range. The bias measurements are processed in-flight by the programmable microcomputer and stored in the on-board OARE memory.

The basic assumption in this process is that during the bias measurements the input signal does not change appreciably. In the laboratory this process can be closely controlled, but not on the Orbiter. In lieu of this, certain experimental steps can be taken to minimize the errors introduced into the process. For example, by keeping the measurement time frame small, by taking a statistically

significant sample, and by monitoring the Orbiter movements, the errors introduced can be kept small enough to meet the experiment objectives. The errors are discussed in a later section.

#### Scale-Factor Calibration

The sensor proofmass is offset from both the inner-gimbal and the outer-gimbal centers of rotation. The  $X$  axis is calibrated by rotation at a constant known rate about the inner gimbal; the  $Y$  and  $Z$  axes are calibrated by rotation about the outer gimbal. The theoretical centripetal accelerations are compared with the measured accelerations, and the scale factors are calculated. Two rotational velocities are used for each axis and range to check the sensor linearity. The length of time for the rotation process and the theoretical induced centripetal calibration acceleration signals are included in Table 1.

#### Calibration Sequence

A typical OARE flight calibration sequence for both biases and scale factors is shown in Fig. 3 as a function of gimbal angle measurements versus mission elapsed time (MET). Typically, the calibration sequence takes a half hour, during which the measurements for the biases and the scale factors for the three axes and the three ranges are performed. On STS-58, 43 complete sequences were collected.

#### Bias Calibration Results

During the STS-58 mission, the root-mean-squared noise of the acceleration signals is about 2 to 4  $\mu g$  for "quiet" times to well above 10  $\mu g$  for "active" times. Active times occur during crew work periods when life-support systems are more active, the crew is involved in experiments, small thrusters are fired, etc. To extract information in this environment, a statistical trimmed-mean filter is used on the measurements taken during the bias calibration.<sup>11</sup> In orbit, the trimmed-mean averaged signals are recorded in the OARE computer memory, along with their statistics ( $1\sigma$  deviations), the MET, and the sensor temperature. Generally, the greatest contributor to the magnitude of the  $1\sigma$  deviations comes from the environment.

The results of these STS-58 OARE measured biases for the  $X$ ,  $Y$ , and  $Z$  axes, along with their respective error bars, are shown in Fig. 4 and can be compared with the results from STS-50 shown in Fig. 5. The  $Y$  and  $Z$  axes show an apparent improvement in errors, but this improvement is only the result of an electronic-filter change for the STS-58 mission. The errors on the  $X$  axis appear significantly larger on STS-58. This result is surprising, since the STS-50 mission had the more rigorous schedule (i.e., red and blue teams working experiments around the clock). More significantly, however, the  $X$  axis has clearly shifted from a negative (STS-50) to a positive (STS-58) bias.

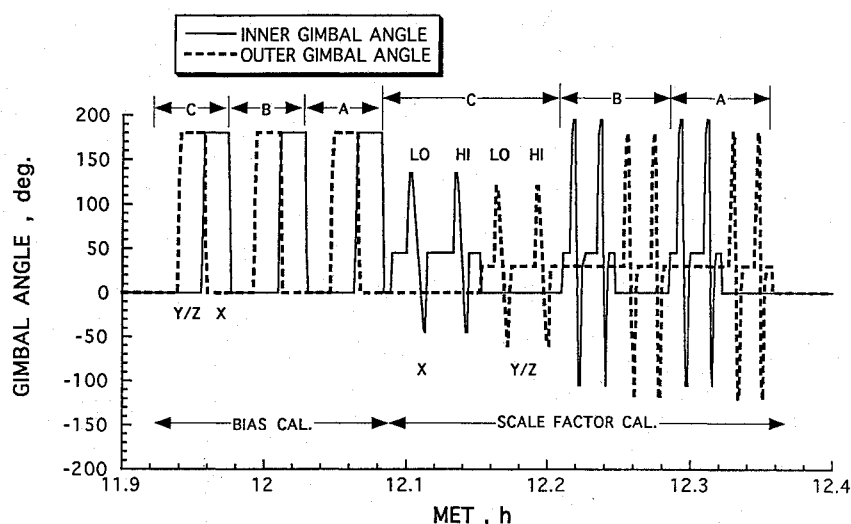


Fig. 3 Typical measurements of inner and outer gimbal angles during a calibration sequence.

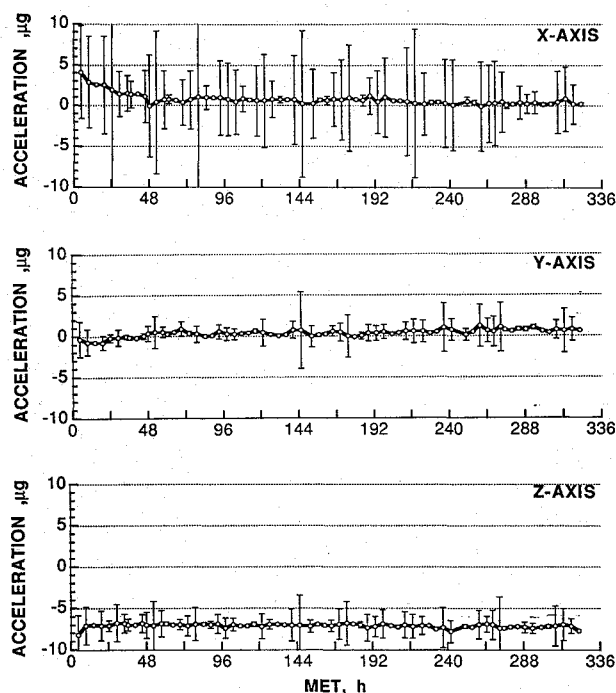


Fig. 4 OARE STS-58 bias measurements with average deviations.

In both Figs. 4 and 5 a noticeable bias drift in all axes occurs at the beginning of each mission for about 40 to 50 h, after which it remains fairly constant. This drift is due to dielectric charging of the ceramic forcer ring assembly and is a characteristic of the sensor.<sup>14</sup> The drift is most pronounced on the X axis.

The temperature sensitivity of the biases for both flights can be seen in Fig. 6. This figure shows clearly the very low bias and temperature sensitivity of the sensor, thus providing an ideal situation for low-frequency acceleration measurements. The interest in showing the comparison of the data between two flights is the long-term behavior. These flights are separated by many months, and the instrument is subjected to severe launch and landing shock, pressure changes from vacuum to sea level, and other severe environmental changes such as temperature and humidity. The only significant change in the bias behavior is for the X axis. Its bias and temperature dependence have changed, whereas very little change can be seen for the Y and Z axes when comparing STS-58 with STS-50. This change in the X axis was probably influenced by the imminent failure of the operations amplifier circuit. This failure occurred after STS-58 data collection was completed and was

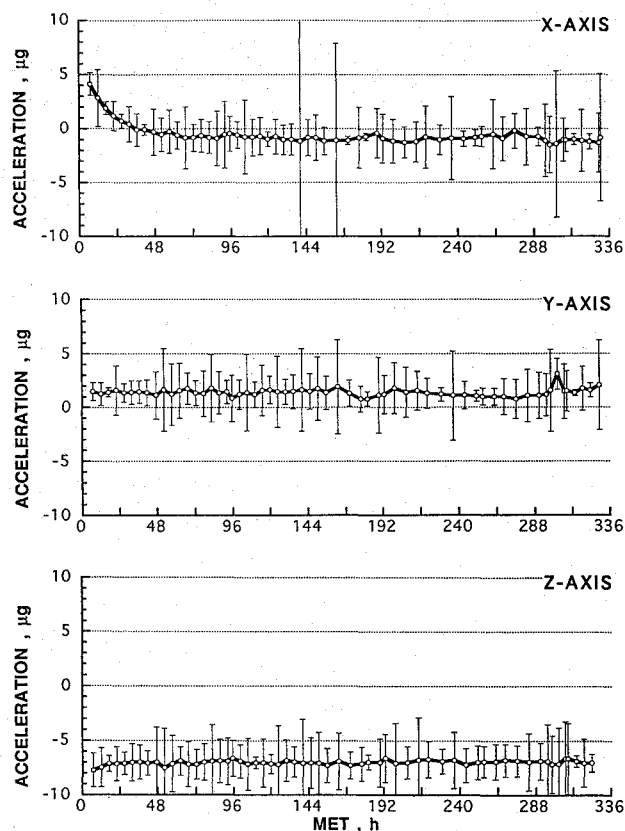


Fig. 5 OARE STS-50 bias measurements with average deviations.

discovered after the instrument was removed from the Orbiter. In general, however, this postflight failure poses no serious problems for further interpretation of absolute acceleration levels for either flight, since the bias behavior is measured frequently throughout both missions.

#### Scale-Factor Calibration Results

As discussed, the on-orbit scale-factor calibration of each sensor axis is accomplished by rotating the proofmass at known rates about one of the two gimbal axes (i.e., the inner-gimbal axis for X-axis calibration, and the outer-gimbal axis for Y- and Z-axis calibration). The distances from gimbal axes to proofmass are known precisely, and the rotation rates are accurately controlled. Thus, the calibration acceleration signal can be calculated within a fraction of one percent. This calibration input signal is referred to as the "theoretical" signal.

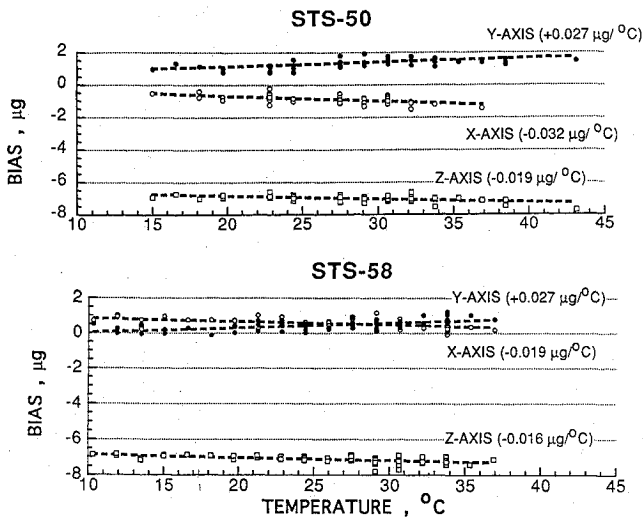


Fig. 6 Comparison of OARE STS-58 in-flight bias temperature-sensitivity measurements with corresponding STS-58 measurements.

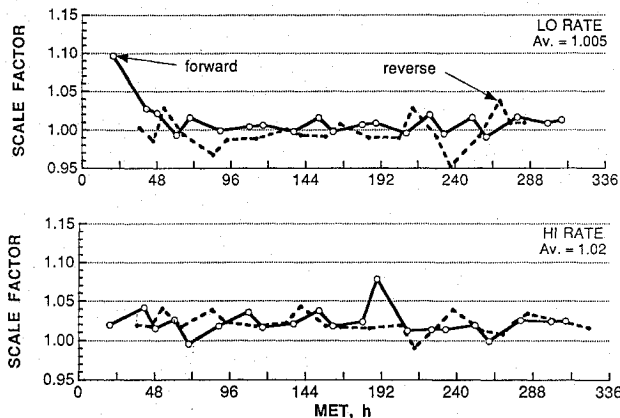


Fig. 7 OARE STS-58 X-axis, C-range scale-factor measurements.

In principle, the reference value obtained when the sensor is not rotating is subtracted from the measured acceleration during rotation. This difference provides the relative acceleration amplitude generated by the platform motion. This amplitude, referred to as the "measured" acceleration, is compared with the theoretical acceleration to define the scale-factor ratio SF, that is,

$$SF = A_{\text{theor}}/A_{\text{meas}} \quad (1)$$

The scale-factor ratio typically has a value near unity. This will be the situation if the counts from the accelerometer, which are initially scaled on each range using the manufacturer's conversion factors, correspond exactly to the theoretical signal produced by the platform rotation. The SF is used as a multiplier adjustment to the acceleration measurements made during flight, after subtracting the bias.

The reference signal is measured at rest at a position halfway through the slew. This reference, therefore, should eliminate all but a small amount of the effects of outside residual acceleration on the determination of the scale-factor ratio. However, these external accelerations, mainly from gravity-gradient and out-of-plane effects, Orbiter rotation, and Coriolis acceleration from simultaneous Orbiter rotation and platform slew rotation, are calculated and are found to alter the scale factor by about 2% in some cases. These effects have been incorporated in the scale-factor data reduction process.

Each range (A, B, or C) for each axis employs a low- and a high-rate slew, which are used to determine the extent that the scale factor varies with acceleration level. In addition, the slew can be in the forward or reverse sense. This direction is recorded for each scale-factor determination so that any direction-dependent effect can be identified.

Figures 7 and 8 are the results of the scale-factor measurements for the C range of the X and Y axes for STS-58. Note that, in the

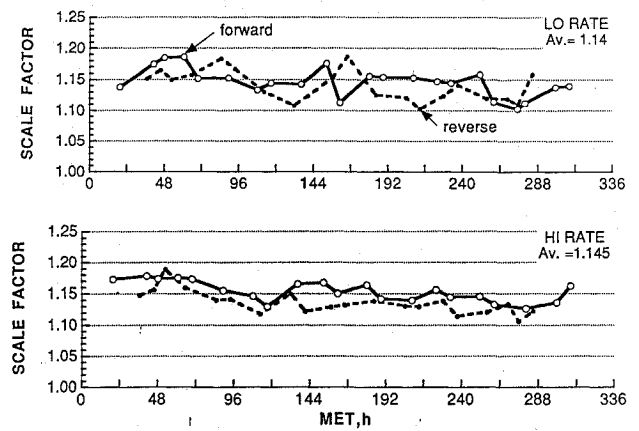


Fig. 8 OARE STS-58 Y-axis, C-range scale-factor measurements.

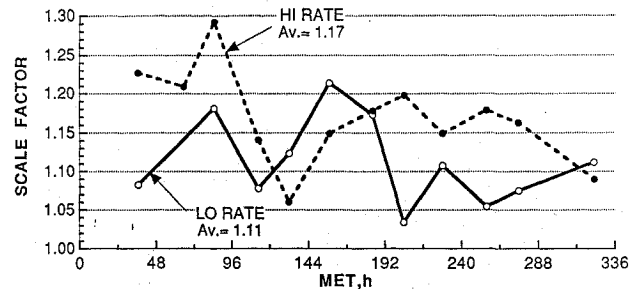


Fig. 9 OARE STS-58 Z-axis, C-range scale-factor measurements (reverse direction).

X-axis case, forward and reverse slews have very little effect on the magnitude of the scale factor, but the scale factor does increase slightly from low to high rate, which may indicate a slight nonlinearity. The Y-axis scale factor changes very little with slew rate, but does appear to decrease slightly throughout the flight for both rates.

For STS-58, the Z axis did not perform properly in the C range during its scale-factor-induced motion. Postflight diagnostics indicate that saturation of the signal conditioner caused by a "jitter" of the motor corrupted the Z-axis signal in the C range. This problem required a special analysis to recover the scale factor for this axis, and details are available.<sup>4</sup> Final results for the Z axis are shown in Fig. 9. The mean scale factor for the reverse-direction low rate is 1.11 and for the reverse-direction high rate is 1.17 (forward-rate data gave unsuccessful results for this axis).

### In-Flight Calibration Maneuvers

The stimulus to an accelerometer for acquiring data to measure the scale factor is usually accomplished by mounting the sensor to a movable platform and rotating it in a controlled fashion. Some laboratories use a centrifuge device for this purpose. This activity is accomplished in orbit with high accuracy using the OARE calibration table, as previously discussed. It can also be accomplished by holding the calibration station at rest and rotating the spacecraft itself at prescribed, measurable rates.

One of the experiment goals of the OARE is to provide validation information for the scale-factor data generated by the calibration table, since this is the first attempt to perform scale-factor measurements in space. A series of Orbiter flight maneuvers were designed in order to stimulate the OARE sensor axes in a predictable manner, in order to validate the calibration station. These Orbiter maneuvers consisted of a series of three 360-deg rotations (i.e., pitch, yaw, and roll) about each of its body axes. On STS-58, three sets of these maneuvers were performed during the mission on MET days 2, 6, and 9. This section reports on the analysis and results from these maneuvers.

### Maneuver Analysis

In principle, spacecraft rotation imitates the OARE calibration-station scale-factor calibration activity, but there are significant differences in the way the measurements are analyzed. First, during

Table 2 Results from OARE flight maneuvers on STS-58

Maneuver no.	MET day	Body axis	Maneuver		
			Pitch	Yaw	Roll
<i>a) Scale factors</i>					
1	2	X	1.07	1.07	—
		Y	—	1.07	0.66
		Z	1.10	—	1.10
2 <sup>a</sup>	6	X	1.07	1.06	—
		Y	—	1.07	1.00
		Z	1.11	—	1.12
3	9	X	1.06	1.05	—
		Y	—	1.08	0.77
		Z	1.11	—	1.11
<i>b) Average induced acceleration, <math>\mu g</math></i>					
1	2	X	67.0	38.6	—
		Y	—	-4.2 <sup>b</sup>	0.59
		Z	-57.5	—	-42.4
2	6	X	71.6	40.0	—
		Y	—	-5.0 <sup>b</sup>	0.56
		Z	-61.4	—	-44.2
3	9	X	72.1	39.8	—
		Y	—	-4.0 <sup>b</sup>	.74
		Z	-61.4	—	-36.9

<sup>a</sup>Aborted during roll maneuver.<sup>b</sup>Large midmaneuver attitude correction.

spacecraft rotation, the OARE instrument encounters changes in aerodynamic and gravitational stimuli. These stimuli must be identified and accounted for in the theoretical signal before scale-factor calculations can be made. These stimuli, as well as inertial coupling, produce small derivatives of the rotation rates, which in turn also affect the theoretical acceleration.

To generate the calibration signal (referred to earlier as the "theoretical" signal) by rotating the spacecraft, the components of the calibration signal are calculated using measurements taken from the Orbiter Data Reduction Complex (ODRC) at Johnson Space Center. These measurements include body rates ( $\omega$ ) and orientation, the position vector (Earth center to Orbiter), and the Orbiter's velocity vector. The vector equation for the theoretical signal is

$$A_{\text{theor}} = A_{\text{aero}} + A_{\text{gg}} + A_{\text{oop}} + \omega \times (\omega \times r) + \dot{\omega} \times r \quad (2)$$

Equation (2) is used to produce the theoretical calibration signals to which the OARE measurements are scaled. These components of the signal include aerodynamic, gravity-gradient, and out-of-plane terms, and terms involving angular rates and accelerations about the Orbiter center of gravity. The out-of-plane component is caused by the OARE sensor's horizontal displacement from the Orbiter's center of gravity. The position of the OARE proofmass within the spacecraft is accurately known from measurements taken during initial installation in the Orbiter. (In the Orbiter coordinate system,  $X_0 = 1153.140$  in.,  $Y_0 = -1.313$  in., and  $Z_0 = 317.932$  in.) The Orbiter center of gravity in the Orbiter coordinate system as a function of mission elapsed time is provided by the Orbiter Project Office. The difference in these two locations establishes  $r$  in the above equation as a function of mission elapsed time. The rotational accelerations  $\dot{\omega}$  (i.e., body-rate derivatives) are defined from piecewise curve fitting and differentiation of  $\omega$  for selected data segments. The measurements obtained from the ODRC, along with predictions of atmospheric density and aerodynamic coefficients, are used to calculate  $A_{\text{aero}}$ ,  $A_{\text{gg}}$ ,  $A_{\text{oop}}$ , and the rotation effects. Typically the magnitudes of  $A_{\text{aero}}$ ,  $A_{\text{gg}}$ ,  $A_{\text{oop}}$  are less than about 0.6, 0.6, and 0.3  $\mu g$ , respectively. Table 2 lists the magnitudes of the average induced accelerations during spacecraft rotation. Clearly, the contributions from these three terms are small relative to the induced signal, and in some cases negligible. Thus, any errors in the calculation of these terms are smaller yet and should not contribute significantly to the overall errors.

Table 3 Maneuver solution

Maneuver	Axis to rotate about	Scale-factor solution axes
Pitch	Y	X, Z
Yaw	Z	X, Y
Roll	X	Y, Z

### Scale-Factor Results

In general, for an accelerometer not on the vehicle center of gravity, Table 3 provides the axes for which scale-factor solutions are possible as a function of spacecraft maneuver. Each maneuver provides data for scale-factor solutions for two axes. Thus, the three maneuvers give two scale-factor solutions for each axis. Ideally, for a perfect instrument (i.e., no nonlinearities or other aberrations), with perfect maneuvers (i.e., no cross-coupling motions or angular accelerations) and error-free angular measurements (i.e., perfect gyros), the solutions would be redundant. In fact, this is not the case, but the multiple solutions provide data from which to judge the reliability of the solutions obtained. Mission STS-58 data are unique in that three sets of maneuvers were performed, allowing six independent solutions per axis to be obtained.

Table 2 summarizes the data resulting from the analysis of the three maneuvers. The table has two parts, namely, a) the scale-factor results for all the maneuvers on STS-58, and b) the average induced accelerations along each axis at the OARE location that are generated by each of the three sets of maneuvers. The scale-factor solution for the  $X_b$  axis yields  $1.06 \pm 0.01$ . Comparing this result with Fig. 7 (the calibration-station scale factor) shows that on the average this value is larger by about 0.05 than the average scale factor measured over the entire mission.

There are two plausible explanations for these differences: 1) there is a slight nonlinearity in this axis over its operating range, or 2) the center of gravity of the Orbiter is off (too far forward) by about 7.5 cm (3 in.). The linearity hypothesis does not appear correct, since the acceleration induced in the  $X$  axis during the high platform rate is very near the acceleration created by the Orbiter yaw motion. Thus, it is highly likely that the tabular center-of-gravity location of the Orbiter is slightly in error. That is, a slight shift of the Orbiter center-of-gravity location, about 7.5 cm (3 in.) aft, would completely resolve the differences in scale factors between the maneuvers and the platform motion.

From Table 2, the scale-factor solution for the  $Y_b$  axis is  $1.075 \pm 0.05$  based upon the yaw maneuvers and  $0.81 \pm 0.2$  based upon the roll maneuvers. These results compare with the calibration-station scale-factor value in Fig. 9 ( $Z$ -sensor axis) of  $1.14 \pm 0.03$ . The most reliable solution is 1.075, since the roll maneuvers did not stimulate the sensor much because of the proximity of the instrument to the center of rotation (see Table 2b). Also, the values obtained from the calibration table are questionable, since they come from a poor-quality signal, as discussed earlier.

The scale-factor solution for the  $Z_b$  axis is  $1.11 \pm 0.01$  as determined from the maneuvers. This result compares with the average value in Fig. 8 ( $Y$  sensor axis) throughout the mission: 1.14. It is quite close, indicating that calibrations for this axis are quite reliable.

### Uncertainty Bounds

On-orbit bias and scale-factor measurements provide the means to produce absolute acceleration measurements. However, both bias and scale-factor determinations on orbit have uncertainties associated with them. Small variations in calibration results can be caused by the inherent imprecision of the instrument, spacecraft motion, and jet firings; additionally, only a limited number of calibrations can be performed during the flight. Thus, the determination of the absolute acceleration is known to within certain limits, which depend directly on how well both the bias and the scale factors have been determined.

### Bias Estimates

Figure 10 contains three graphs of the standard error along each of the OARE sensor axes for each of the bias measurements taken on STS-58. The standard error is calculated in the following manner:

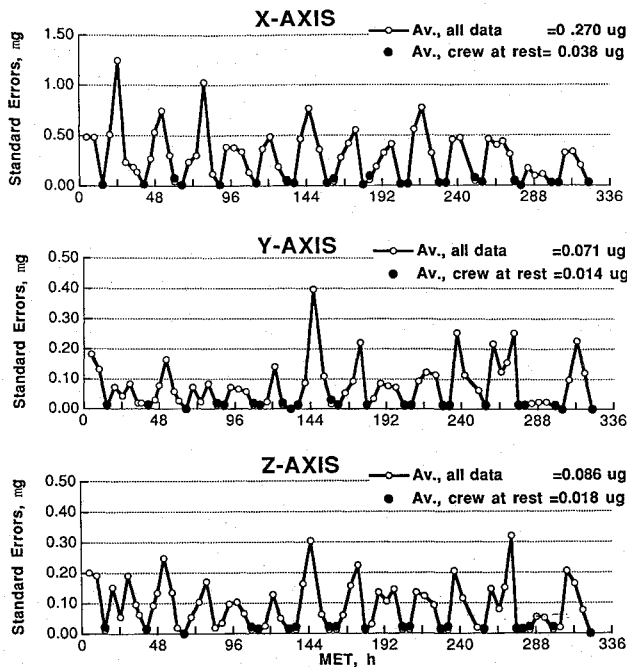


Fig. 10 STS-58 in-flight bias measurements: average standard errors.

Each bias measurement contains two separate, independent sets of measurements, one in a given direction and another 180 deg opposite to that direction. A trimmed-mean filter is applied to each set of these measurements separately, resulting in a mean and a standard deviation. The average of the standard deviations is calculated, and the central limit theorem<sup>15</sup> is applied.

There are two average standard errors given on each graph in Fig. 10. The larger number is the statistic obtained by using all 69 measurements, and the smaller number is obtained by using the values when the crew was asleep (data with the filled-in circles). This subset of measurements is of superior quality and is more indicative of the true capabilities of the OARE calibration system.

Finally, it is clear that the standard error is a function of the OARE internal electronic filters. The X-axis errors are three times larger than the Y- or Z-axis errors. The smaller errors on these axes are results of the internal electronic smoothing process intentionally introduced for the Y and Z axes to eliminate the platform jitter during scale-factor activities.

#### Scale-Factor Estimates

Figure 11 contains three graphs of the standard error along each of the OARE sensor axes for each of the scale-factor measurements taken on STS-58. The standard error is calculated in the same manner as the bias standard error, with a few exceptions. First, there are three sets of data per scale-factor measurement, namely, a set of measurements before, during, and after platform motion. Thus the average involves three standard deviations instead of two, as used for calculating the bias errors. The other consideration is that each Z-axis data set was individually inspected; data and entire sets were removed, thus affecting the statistics.

Again, examining Fig. 11, the quiet periods during astronauts' sleep provide the ideal time to perform the calibration measurements. These data are indicated by the filled-in circles on each graph in the figure, and the average is significantly smaller than the average taken over the entire mission. The X-axis errors are again significantly larger than those for both Y and Z axes, as a result of internal smoothing, as explained earlier.

#### Estimates During Maneuvers

The errors associated with determining scale factors from the maneuvers are complex, since they come from several sources, namely measurement errors (e.g., in the body rates and angular accelerations, the center-of-gravity location, the sensor location) and model errors (e.g., in the aerodynamic coefficients, density, and angular

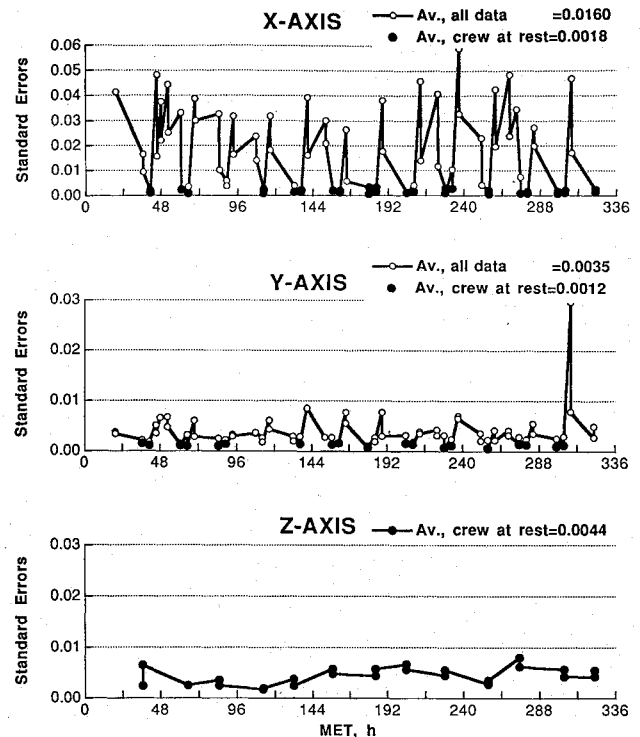


Fig. 11 STS-58 in-flight scale-factor measurements: average standard errors.

orientations for gravity-gradient effects). In lieu of a formal error analysis, this article provides an estimate of the error bounds by examining the variations in the scale-factor solutions shown in Table 2. There are six scale-factor solutions per axis, and the variations for the scale factor are  $\pm 0.01$ ,  $\pm 0.21$ , and  $\pm 0.01$  for the X, Y, and Z axes, respectively. The Y-axis variation is the largest, mainly because of the poor solutions during the roll maneuver (very short lever arm for this axis). Neglecting these solutions would provide a variation approximately equivalent to that obtained for the other two axes.

#### Conclusions

The OARE, an accelerometer system with  $10^{-9}$  g sensitivity and in-flight calibration capability, has flown on three development flights: STS-40, -50, and -58. Detailed analyses of measurements of both the in-flight bias and the scale-factor in the C range (the most applicable range while in orbit) for STS-58 have been performed.

On STS-58, the Y- and Z-axis bias results matched closely the data obtained on the previous flight, STS-50. The X axis indicated a significant change between flights, but, subsequent to the STS-58 mission, a major electronic component failed, suggesting an influence in the operation of the sensor during that flight. In perspective, however, the Y- and Z-axis bias results show no significant change in magnitude or change in temperature sensitivity. This result provides the first evidence of system robustness when subjected to shock, severe environment changes, and a considerable passage of time between flights.

The calibration-station scale-factor results on all three axes were obtained throughout the entire flight. A detailed analysis of three sets of pitch, yaw, and roll maneuvers of the Orbiter was also made so as to verify the calibration-station scale-factor results. This analysis is particularly valuable in that this is the first time on-orbit scale-factor determinations have been performed on the Orbiter.

Along the X axis, there is a difference of about 5% between the average scale factor as determined with data from the calibration station and the data determined from the maneuvers, i.e., 1.01 vs 1.06, respectively. This difference may be partly attributable to misinformation on the location of the Orbiter's center of gravity, since a change of only 7.5 cm would account entirely for the difference. The Y-axis scale factor determined by the calibration station is in excellent agreement with the maneuver data. On this axis, there is a

slight time dependence (decrease) in the scale factor over the 14 days of measurements. The average value over the flight as determined from the calibration stations is slightly higher (by about 3%) than that obtained from the maneuvers, i.e., 1.14 vs 1.11, respectively. This difference is again mostly attributable to the lack of knowledge of the location of the Orbiter center of gravity. The Z-axis scale factor as determined by the maneuvers provides more reliable information than the poor-quality data given by the calibration station. There was a problem with the Z-axis scale-factor calibration due to jitter during platform motion, which caused a significant deterioration of the results on this axis. The average scale factor for this axis determined from data from platform motion is 1.14. At present, the more reliable scale factor, 1.075, is that determined during maneuvers.

The combined STS-58 on-orbit bias and scale factors provide the means to achieve an absolute measurements of the residual acceleration on the Orbiter on orbit. This measurement is orders of magnitude superior to those from past Orbiter pendulous accelerometer systems, such as HiRAP. Specifically, HiRAP bias ground calibrations yield an absolute measurement uncertainty on the order of 80  $\mu\text{g}$ , and flight techniques used to improve this uncertainty bring it down to the order of 5  $\mu\text{g}$ ; for OARE, the corresponding uncertainty is about 0.04  $\mu\text{g}$ . This improved performance should directly benefit both national and international on-orbit experimenters.

## References

- <sup>1</sup>Blanchard, R. C., Hendrix, M. K., Fox, J. C., Thomas, D. J., and Nicholson, J. Y., "The Orbital Acceleration Research Experiment," *Journal of Spacecraft and Rockets*, Vol. 24, No. 6, 1987, pp. 504-511.
- <sup>2</sup>Anon., "ACIP/HiRAP End Item Specification," Bendix Corp., Aerospace Systems Div., Drawing No. 3291583, Ann Arbor, MI, May 1982.
- <sup>3</sup>Blanchard, R. C., and Rutherford, J. F., "The Shuttle Orbiter High Resolution Accelerometer Package Experiment: Preliminary Flight Results," *Journal of Spacecraft and Rockets*, Vol. 22, No. 4, 1985, p. 474.
- <sup>4</sup>Blanchard, R. C., Nicholson, J. Y., Ritter, J. R., and Larman, K. T., "OARE Flight Maneuvers and Calibration Measurements on STS-58," NASA TM-109093, Apr. 1994.
- <sup>5</sup>Blanchard, R. C., Larman, K. T., and Moats, C. D., "Flight Calibration Assessment of HiRAP Accelerometer Data," AIAA Paper 93-0836, Jan. 1993.
- <sup>6</sup>Anon., "Microgravity Science and Applications Program Tasks," 1991 rev., NASA-TM-4349, Feb. 1992.
- <sup>7</sup>Ott, R., "NASA's Commercial Microgravity Program," AIAA Paper 93-0371, Jan. 1993.
- <sup>8</sup>Wetter, B., "Canada's Microgravity Science Program," AIAA Paper 93-0372, Jan. 1993.
- <sup>9</sup>Latorre, R., and Mims, J., "Soviet Approach to Space Manufacturing in Microgravity," AIAA Paper 93-0375, Jan. 1993.
- <sup>10</sup>Rogers, M. J. B., Baugher, C. R., Blanchard, R. C., DeLombard, R., Durgin, W. W., Matthiesen, D. H., Neupert, W., and Roussel, P., "Low Gravity Environment On-board Columbia During STS-40," AIAA Paper 93-0833, Jan. 1993.
- <sup>11</sup>Blanchard, R. C., Nicholson, J. Y., and Ritter, J. R., "STS-40 Orbital Acceleration Research Experiment Flight Results During a Typical Sleep Period," *Microgravity Science and Technology*, Vol. 2, July 1992, pp. 86-93.
- <sup>12</sup>Blanchard, R. C., Nicholson, J. Y., and Ritter, J. R., "Preliminary OARE Absolute Acceleration Measurements on STS-50," NASA TM-107724, Feb. 1993.
- <sup>13</sup>Anon., "Aerodynamics Design Substantiation Report—Vol. I: Orbiter Vehicle," Rockwell International, Space Division, Downy, CA, SD74-SH0206-1H, Jan. 1986.
- <sup>14</sup>McNally, P. J., and Blanchard, R. C., "Comparison of OARE Ground and In-flight Bias Comparisons," AIAA Paper 94-0436, Jan. 1994.
- <sup>15</sup>Snadecor, G. W., and Cochran, W. G., *Statistical Method*, 7th ed., Iowa State Univ. Press, 1980, pp. 45-50.

I. D. Boyd  
Associate Editor